Journal of the Mechanical Behavior of Biomedical Materials 88 (2018) 322–329

Contents lists available at ScienceDirect

Journal of the Mechanical Behavior of Biomedical Materials

journal homepage: www.elsevier.com/locate/jmbbm

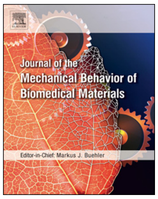

The role of water in the initial sliding of nacreous tablets: Findings from the torsional fracture of dry and hydrated nacre

Saleh Alghamdi[a,d], Fen Du[b], Jie Yang[c], Ting Tan[a,*]

[a] Department of Civil and Environmental Engineering, University of Vermont, 33 Colchester Avenue, Burlington, VT 05405, USA
[b] Department of Mechanical Engineering, Vermont Technical College, Randolph Center, 201 Lawrence Pl, VT 05061, USA
[c] Department of Physics, University of Vermont, 82 University Place, Burlington, VT 05405, USA
[d] Department of Civil Engineering, Taif University, Taif 21974, Saudi Arabia

ARTICLE INFO

Keywords:
Nacre
Water
Fracture
Nanoscale toughening mechanisms
Laminated nanomaterials
Torsion

ABSTRACT

Nacre exhibits remarkable mechanical properties resulting from its hierarchical brick-and-mortar structures. By using pure shear stresses of torsion, we demonstrate how nacre resists the initial tablet sliding by tuning its nanoscale toughening mechanisms in dry and hydrated conditions. In hydrated nacre, hydrogen bonds between water molecules and organic matrices provide temporal paths for stress redistributions, through which the shear resistance is gradually transferred from mineral bridges to contacted nanoasperities. In the subsequent sliding, dynamical interactions between nacreous tablets enable substantial plasticity before the catastrophic failure of hydrated nacre. Our findings should help pursuing further insights into the interfacial behavior of natural and artificial laminated nanomaterials under different conditions.

1. Introduction

Nacre, a composite made from aragonite and organic matrices, exhibits extraordinary strength and toughness due to its hierarchical brick-and-mortar structures (Askarinejad and Rahbar, 2015; Barthelat et al., 2016; Currey, 1977; Currey et al., 2001; Gao et al., 2003; Gu et al., 2017; Jackson et al., 1988; Li et al., 2006, 2004; Liu et al., 2012; Meyers et al., 2008a; Ortiz and Boyce, 2008; Sarikaya et al., 1989; Shao et al., 2014; Wegst et al., 2015; Wise Jr, 1970; Xu et al., 2013; Zhang et al., 2011). When nacre is hydrated, its mechanical behavior is different from that of the dry nacre. Prior studies revealed that the hydrated nacre exhibited larger strain than that of dry nacre under tension (Barthelat and Espinosa, 2007; Barthelat et al., 2007; Song et al., 2008; Verho et al., 2018; Wang et al., 2001), bending (Verho et al., 2018; Wang et al., 2001), direct shear (Barthelat and Espinosa, 2007; Barthelat et al., 2007) and 45° shear tests (Barthelat and Espinosa, 2007; Barthelat et al., 2007; Wang et al., 2001). It has been reported that the fractured hydrated nacre exhibits more pulled-out nacreous tablets, whereas the fractured dry nacre exhibits more broken tablets (Richter et al., 2011). These differences are strongly dependent on the performance of the aragonite tablets and organic matrices composed of chitin (N-acetylglucosamine) networks and different proteins (Dubey and Tomar, 2010; Launspach et al., 2012; Schaffer et al., 1997; Zentz et al., 2001). By performing Fourier-transform infrared spectroscopic analysis, Verma et al. (2007) revealed that there are different forms of water in hydrated nacre, including the partially hydrogen bonded water with organic matrices, the fully hydrogen bonded water clusters inside organic matrices or aragonite tablets, and the chemisorbed water on the tablet surfaces. Meanwhile, different nanoscale toughening mechanisms (Askarinejad and Rahbar, 2015; Li et al., 2006; Meyers et al., 2008a; Smith et al., 1999; Wang and Gupta, 2011; Wegst et al., 2015) have been identified between nacreous tablets, including mineral bridges, nanoasperities and protein chains, which have been evidenced by microscopic imaging in the static condition (Meyers et al., 2008b; Su et al., 2002; Yao et al., 2009). Furthermore, proofs have been obtained for the sudden breakage of mineral bridges (Alghamdi et al., 2017) and the unfolding and deformation-strengthening of protein chains (Smith et al., 1999; Xu and Li, 2011) through stress-strain curves. Despite these studies, limited research exists to elucidate how water affects the nanoscale interfaces between nacreous tablets compared to that of the dry nacre during the initial sliding. Also, the experimental evidence of how nanoasperities interact with each other dynamically or how different nanoscale toughening mechanisms evolve as the nacreous tablets slide are scarce.

One primary challenge to explicitly display the evolution of nanoscale toughening mechanisms between nacreous tablets is to isolate the sliding of two adjacent tablets from the rest of the brick-and-mortar structure. The discretizational nature of torsion (Tan et al., 2013; Wang

---

[*] Corresponding author.
E-mail address: ting.tan@uvm.edu (T. Tan).

https://doi.org/10.1016/j.jmbbm.2018.08.051
Received 17 August 2018; Received in revised form 27 August 2018; Accepted 30 August 2018

1751-6161/ Published by Elsevier Ltd.

et al., 2015; Zhou et al., 2015) could reveal the behavior of two nacreous tablets in the initial nanoscale sliding. In torsion, two-dimensional planes of pure shear stresses are stacked along the longitudinal axis. If nacre is treated as transversely isotropic, the shear stress distribution along the radius is linear before the specimen fails (See Supplementary materials, Fig. S1). Due to the differences between nacreous tablets and the nanogaps (~ 30 nm) in between (Meyers et al., 2008a), the mismatch of shear stresses causes nacre to fail through the tablet interfaces. Because the polar moment of inertia decreases substantially once the interface between the surface tablets fail, the stress gradients along the radius fail the inside tablet interfaces rapidly. The shear stress and strain in torsion are described by

$$\tau = \frac{T\bullet\rho}{J} \tag{1}$$

$$s_m = \Delta\theta\bullet r = \gamma_m\bullet l \tag{2}$$

Where τ is the shear stress on the horizontal plane of the gauge section, T is the torque, r is the gauge section radius, ρ is the distance between an arbitrary point on the cross section to the center varying from 0 to r, $J = 0.5\pi r^4$ is the polar moment of inertia, γ_m is the surface shear strain, s_m, $\Delta\theta$, and l are the surface sliding distance, twisting angle, and the height of adjacent tablets, respectively. The surface sliding distance upon failure is measured as the rotational distance between two adjacent tablets on the cylindrical surface. The surface shear strain is the angle between the sliding distance and the height of adjacent tablets. The primary goal of this work is to elucidate how hydrated nacre exhibits different mechanical behaviors from dry nacre in the initial sliding by tuning the nanoscale toughening mechanisms. We do not further distinguish the roles of different types of water in hydrated nacre. We performed fractural experiments under torsion with high temporal resolution measurements, and used pure stresses to detail the microstructural interactions between nacreous tablets during the initial sliding. We discussed these findings with finite element simulations and statistical analyses of the minute structural variations at nanoscale.

2. Materials and methods

2.1. Materials

Two red abalone shells with the diameters of ~ 210 mm and ~ 160 mm (The Shell shop, CA, US) were obtained to prepare the dry and hydrated nacre specimens, respectively. Hydrated nacre samples were submerged in distilled water for four weeks before being tested out of water. Both dry and hydrated nacre samples have pure nacreous gauge sections that are devoid of growth lines (Meyers et al., 2008a).

2.2. Specimen preparations

Dog-bone shaped specimens with diameters of 2.6 ± 0.2 mm and gauge section lengths of 2.4 ± 0.0 mm were prepared by aligning the cylindrical axes perpendicular to the polygonal surfaces of nacreous tablets (Fig. 1b). The shells were first cut to cubes with lengths of ~ 7.6 mm. Epoxy segments (Loctite Fixmaster, Rocky Hill, CT) were then added to cube ends to increase the gripping areas. Using a modified lathe, the gauge sections of dog-bone specimens were machined with transition areas. Sample surfaces were polished using 400–7000 grit sandpapers (3M Company, Maplewood, Minnesota). Due to the scarce of pure nacre sections, a total of six dry nacre specimens and three hydrated nacre specimens were created. The match between the discretizational feature of torsion and the microstructure of nacre enables a detailed illustration of the nanoscale interfacial behavior between nacreous tablets using relatively large specimens.

2.3. High temporal resolution experimental systems

An experimental system was created by coupling two load cells to collect the torque-rotation curves at ultrahigh sampling rates (Fig. S1). A small torsional load cell was mounted on top of a large axial-torsional load cell with a maximum torque of 56.5 Nm and a maximum axial load of 4.5 kN (Admet, Norwood, MA). Two types of small load cells were used, i.e., a 2.8 Nm load cell (Futek, Irvine, CA) and a 1.0 Nm load cell (Kistler, Winterthur, Switzerland). Torques from the large load cell were collected at 50 points per second using MtestQuatro (Admet, Norwood, MA), whereas torques from the small load cell were collected at 200,000 points per second using the U2531A data acquisition unit (Keysight Technologies, Santa Rosa, CA). The ultrahigh sampling rate used for the small load cell can record the tiny stress variations caused by the microstructural interactions. The integrated system was well calibrated, of which the linear fitting values (R^2) were 1.0 for the torque ranging from 0.0025 to 1.0 Nm. The rotation of the gauge section was calculated by subtracting rotations from the transition segments and the small load cell from the total rotation measured (Eqs. S1 and S2). Results show that the rotation of the gauge section is ~ 92% of the total rotation measured. Due to the laminated microstructure of nacre, the rotation of the gauge section is discretized to obtain the rotation of two adjacent surface tablets along the longitudinal axis, which was used to calculate the nanoscale sliding distance between them. Special fixtures with four-independent jaws were created to load the dog-bone specimens successfully, in which samples were securely held by two pairs of orthogonal surfaces. Each jaw moved freely to make sure that samples were centered along with the loading axis. To fully disclose the interfacial behavior between nacreous tablets, quasi-static, monotonic, torsional tests were performed to fail dry and hydrated specimens at the displacement rate of 90° per minute. A pre-torque of ~ 0.023 Nm was applied in the torsional test, and a constant tensile force of ~ 0.22 N was applied during the test. The resulting tensile stress was ~ 35 kPa that was far below the tensile strength across nacre tablets (Meyers et al., 2008a). In total, five dry nacre tests were tested using the Futek small load cell. One dry and three hydrated nacre tests were tested using the Kistler small load cell. Consistent results were obtained between different load cells.

2.4. Microscopic characterization

Scanning electron microscopes were used to characterize the fractural surfaces of dry and hydrated nacre specimens. Fractured samples were sputter-coated with gold/palladium film without polishing the surfaces. The coated samples were examined using JEOL 6060 Scanning Electron Microscope (JEOL USA, Peabody, MA) at the beam voltages of ~ 20 kV.

2.5. Wiener filtering

Wiener filter (Antonaglia et al., 2014; Gershenfeld, 1999) was used to reduce the noise at high frequency of stress-strain curves collected at 200,000 points per second. The filter minimizes the differences between the observed and the true signals by eliminating the noise in the frequency domain (Eq. S3) (Gershenfeld, 1999).

3. Results and discussion

The surface shear stress-strain curves for dry and hydrated nacre specimens under monotonic torsional tests are shown in Fig. 1. Because the data from the small load cell was collected at 200k points per second, corresponding stress-strain curves were capable of recording the minute variations in the microstructure. In the dry nacre, the stress-strain curve has an increase stage and a sharp decrease stage (Fig. 1a). The R^2 values of the increase segments are above 0.99 for all six dry specimens, meaning that the failures occurred almost at the end of the linear stage